sensors

MDPI

Article

Heart Rate Variability Analysis on Electrocardiograms, Seismocardiograms and Gyrocardiograms of Healthy Volunteers and Patients with Valvular Heart Diseases

Szymon Sieciński *, Ewaryst Janusz Tkacz and Paweł Stanisław Kostka

Department of Biosensors and Processing of Biomedical Signals, Faculty of Biomedical Engineering, Silesian University of Technology, F. D. Roosevelta 40, 41-800 Zabrze, Poland
* Correspondence: szymon.siecinski@polsl.pl; Tel.: +48-32-277-74-63

Abstract: Heart rate variability (HRV) is the physiological variation in the intervals between consecutive heartbeats that reflects the activity of the autonomic nervous system. This parameter is traditionally evaluated based on electrocardiograms (ECG signals). Seismocardiography (SCG) and/or gyrocardiography (GCG) are used to monitor cardiac mechanical activity; therefore, they may be used in HRV analysis and the evaluation of valvular heart diseases (VHDs) simultaneously. The purpose of this study was to compare the time domain, frequency domain and nonlinear HRV indices obtained from electrocardiograms, seismocardiograms (SCG signals) and gyrocardiograms (GCG signals) in healthy volunteers and patients with valvular heart diseases. An analysis of the time domain, frequency domain and nonlinear heart rate variability was conducted on electrocardiograms and gyrocardiograms registered from 29 healthy male volunteers and 30 patients with valvular heart diseases admitted to the Columbia University Medical Center (New York City, NY, USA). The results of the HRV analysis show a strong linear correlation with the HRV indices calculated from the ECG, SCG and GCG signals and prove the feasibility and reliability of HRV analysis despite the influence of VHDs on the SCG and GCG waveforms.

Keywords: heart rate variability analysis; electrocardiography; seismocardiography; gyrocardiography; valvular heart diseases

Citation: Sieciński, S.; Tkacz, E.J.; Kostka, P.S. Heart Rate Variability Analysis on Electrocardiograms, Seismocardiograms and Gyrocardiograms of Healthy Volunteers and Patients with Valvular Heart Diseases. *Sensors* **2023**, *23*, 2152. https://doi.org/10.3390/s23042152

Academic Editor: Jinseok Lee

Received: 26 December 2022
Revised: 3 February 2023
Accepted: 13 February 2023
Published: 14 February 2023

1. Introduction

Cardiovascular diseases remain the most common cause of death in the world and constitute a significant concern for public health due to the economic burden (expected to reach 47 trillion USD by 2030) and the overload on medical personnel (17.9 million deaths worldwide in 2016) despite progress in prevention, diagnosis and therapy [1–5]. Due to its growing prevalence and significant impact on quality of life [6], we consider valvular heart disease (VHD) in this study.

Valvular heart disease is any cardiovascular disease that affects any heart valve (the aortic valve, mitral valve, pulmonic valve and tricupsid valve) [7,8]. The main causes of VHDs are rheumatic heart disease and ageing [6,8–10]. The most prevalent VHD is aortic stenosis (AS), which is the third most common cardiovascular disease after hypertension and coronary artery disease, and is usually caused either by degenerative calcification of the aortic valve or progressive stenosis of a congenital bicuspid valve [8].

VHDs are usually diagnosed by echocardiography, computed tomography or magnetic resonance imaging [9], which are not feasible in outpatient monitoring [11]. This problem has been addressed by applying various methods [12,13], including exercise electrocardiography (ECG) [14], seismocardiography (SCG) or gyrocardiography (GCG), which register the current mechanical function of the heart with an inertial measurement unit (IMU) placed on the chest wall [11,15,16].

Seismocardiography (SCG) and gyrocardiography (GCG) are two complementary techniques [15,17,18]; seismocardiography is a technique for registering low-frequency precordial acceleration, invented by Bozhenko in 1961 [19,20], whereas gyrocardiography registers the rotational component of cardiac vibrations and was invented by Meriheinä et al. in 2015 [15,16,18,21,22].

Seismocardiographic (SCG) and gyrocardiographic (GCG) signals are non-stationary signals with distinct quasiperiodic features known as waves, e.g., the mitral valve opening wave (MO), the mitral valve closure wave (MC), the isovolumetric contraction wave, the rapid ejection wave, the aortic valve opening wave (AO), the aortic valve closure (AC) wave and the cardiac filling wave [18,22–28]. Figure 1 presents an annotation of concurrent ECG, SCG and GCG signals in a healthy subject.

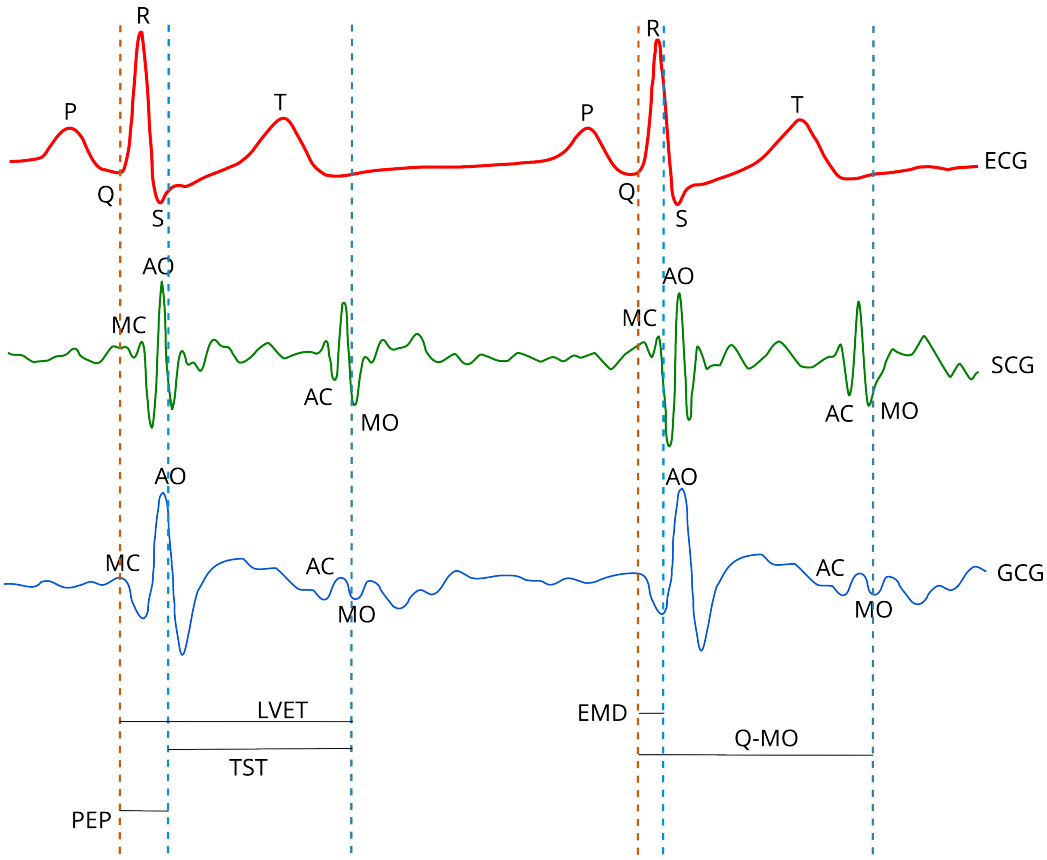

Figure 1. The annotation of ECG, SCG and GCG waveforms in healthy subjects. Based on the diagrams published in [15,18,26,29] under the CC-BY 4.0 license.

SCG and GCG have found applications in the diagnosis of several cardiovascular diseases, such as aortic stenosis [30–32], aortic valve disease (AVD) [33], coronary artery disease [34], myocardial infarction [35,36], atrial fibrillation [37–40], the effects of cardiac resynchronization therapy [41] and heart failure [35,42]. This has usually involved the use of computational intelligence techniques, such as artificial neural networks (including deep and convolutional neural networks), random forests, extreme gradient boosting and support vector machines [28,30,32,35–40].

One of the most prominent applications of seismocardiography and gyrocardiography is heart rate variability (HRV) analysis [16,18,22,31,43–55]. Heart rate variability is defined as the physiological variation in the intervals between consecutive heartbeats (inter-beat interval) and reflects the activity of the autonomic nervous system [56–58].

HRV analysis has traditionally been performed on interbeat intervals obtained from electrocardiograms (ECG signals) [22,43,45,50,51,55,56,59]. The first attempt of HRV analysis based on cardiac mechanical signals (mechanocardiograms) was performed by Friedrich

et al. in 2010 [60] on ballistocardiograms. In 2012, Ramos-Castro et al. performed the first HRV analysis on seismocardiograms [43], and the first HRV analysis on gyrocardiograms was performed by Lahdenoja et al. [61] in 2016. The validity of HRV indices obtained from the SCG signal was first demonstrated by Laurin et al. [62] in 2013 and then in later studies [22,45,46,51–55].

The advantages of using seismocardiography and/or gyrocardiography over electrocardiography for cardiac diagnosis are the simpler measurement setup (using only one sensor) and the availability of information on cardiac intervals, contractility and the state of heart valves at the same time [11,16,22,27,43–45,51,53,56,59,63]. However, the limitations of SCG and GCG include the inter-subject variability of signal morphology that can be significantly affected by cardiac diseases or sensor placement and susceptibility to motion artifacts [11,16,23,27,55,64].

The purpose of this study is to evaluate the differences between the time domain, frequency domain and nonlinear HRV indices derived from electrocardiograms, seismocardiograms and gyrocardiograms in healthy volunteers and patients with valvular heart diseases. This study is an extended version of [54] and is based on two publicly available datasets obtained from healthy people and patients with VHDs.

2. Materials and Methods

2.1. Datasets

This study was carried out on two publicly available datasets with concurrent electrocardiograms, seismocardiograms and gyrocardiograms. The first dataset if "Mechanocardiograms with ECG reference" published by M. Kaisti et al. [65,66] containing signals acquired from twenty-nine healthy volunteers and the second contains thirty signals derived from "An Open-access Database for the Evaluation of Cardio-mechanical Signals from Patients with Valvular Heart Diseases" published by C. Yang et al. in [11,67].

The first dataset consists of 29 recordings of concurrent ECG, SCG and GCG signals acquired from 29 healthy male volunteers that were registered with sensors attached to the chest wall over the sternum with a double-sided tape and with a sampling frequency of 800 Hz. The subjects were lying either in the supine position or on their left or right side [61,65,66].

Electrocardiograms were acquired with an ADS1293 (Texas Instruments, Dallas, TX, USA), seismocardiograms were recorded with a triaxial capacitive digital accelerometer (MMA8451Q from Freescale Semiconductor, Austin, TX, USA) and gyrocardiograms were acquired using a 3-axial MAX21000 gyroscope (Maxim Integrated, San Jose, CA, USA) [15,65].

The rotation and translation axes in seismocardiography and gyrocardiography were defined for both datasets as follows: the x axis was oriented laterally from left to right, the y axis was oriented from head to foot and the z axis was oriented from back to chest [65].

The second dataset consists of 100 simultaneous recordings of raw ECG, SCG and GCG signals with annotated heartbeats acquired from 100 patients with valvular diseases admitted to two different clinical sites: 30 patients were admitted to Columbia University Medical Center (New York City, NY, USA) and 70 patients were admitted to the First Affiliated Hospital of Nanjing Medical University (Nanjing, Jiangsu Province, People's Republic of China). ECG, SCG and GCG signals were recorded before any treatment in both populations of patients [11].

To balance the number of healthy volunteers and patients with valvular heart disease in this comparison study, we took only 30 patients (14 female and 16 male subjects) who were admitted to the Columbia University Medical Center (New York City, NY, USA). A total of thirty patients had aortic stenosis, nine patients had tricupsid valve regurgitation (TR), five had mitral valve stenosis (MS), four had mitral valve regurgitation (MR) and no patients had aortic valve regurgitation. During registration, each subject was asked to be awake and stay in the supine position, breathing normally.

The ECG, SCG and GCG signals were recorded with Shimmer 3 ECG module (Shimmer Sensing, Dublin, Ireland) with a sampling frequency of 256 Hz (recordings UP-01 to UP-

21) and 512 Hz (recordings UP-22 to UP-30) [11,67]. The shimmer 3 device contains a 3-axial inertial measurement unit that contains an accelerometer, a gyroscope and a magnetometer (ICM-20948 from TDK InvenSense, San Jose, CA, USA) and a separate low-noise 3-axial Kionix KXTC9-2050 accelerometer (Kionix, Inc., Ithaca, NY, USA) [68]. Before the measurements, each subject gave informed consent by signing a consent form. All metadata were deidentified before publication [11,67].

The basic characteristics of both datasets are shown in Table 1. Figures 2 and 3 present a 15-second and 16-second fragment of raw ECG, SCG and GCG signals in subject 10 from the first dataset and UP-13 of the second dataset, respectively. More details are revealed in Appendix A.

Table 1. Basic characteristics of the datasets. Aggregated values are expressed as the range (min–max) and mean ± SD.

Dataset	Number of Subjects	Age (Years)	Height (cm)	Weight (kg)	BMI (kg/m^2)	Recording Time (min)
Healthy population	29 male	23–41 29 ± 5	170–190 179 ± 5	60–98 76 ± 11	18–30 24 ± 3	253
VHD patients	14 female 16 male (30 in total)	68–97 83 ± 8	140–183 163 ± 12	44–118 74 ± 17	19–40 28 ± 6	174.8

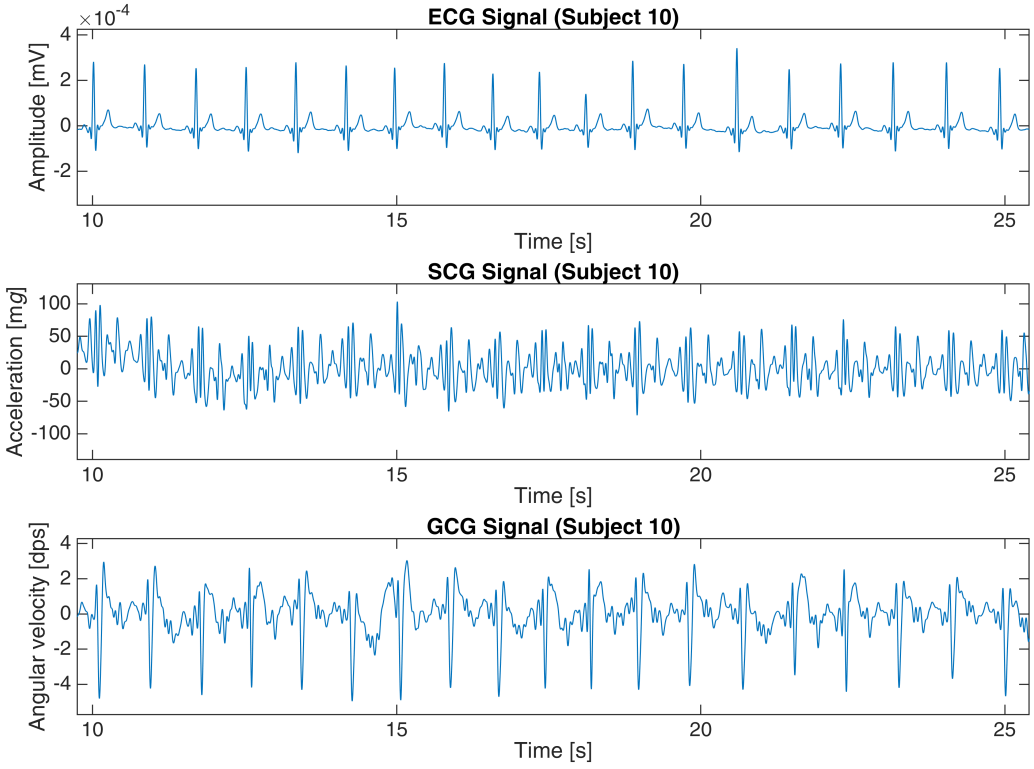

Figure 2. ECG, SCG and GCG signals from subject 10 in the first dataset (25-s fragment).

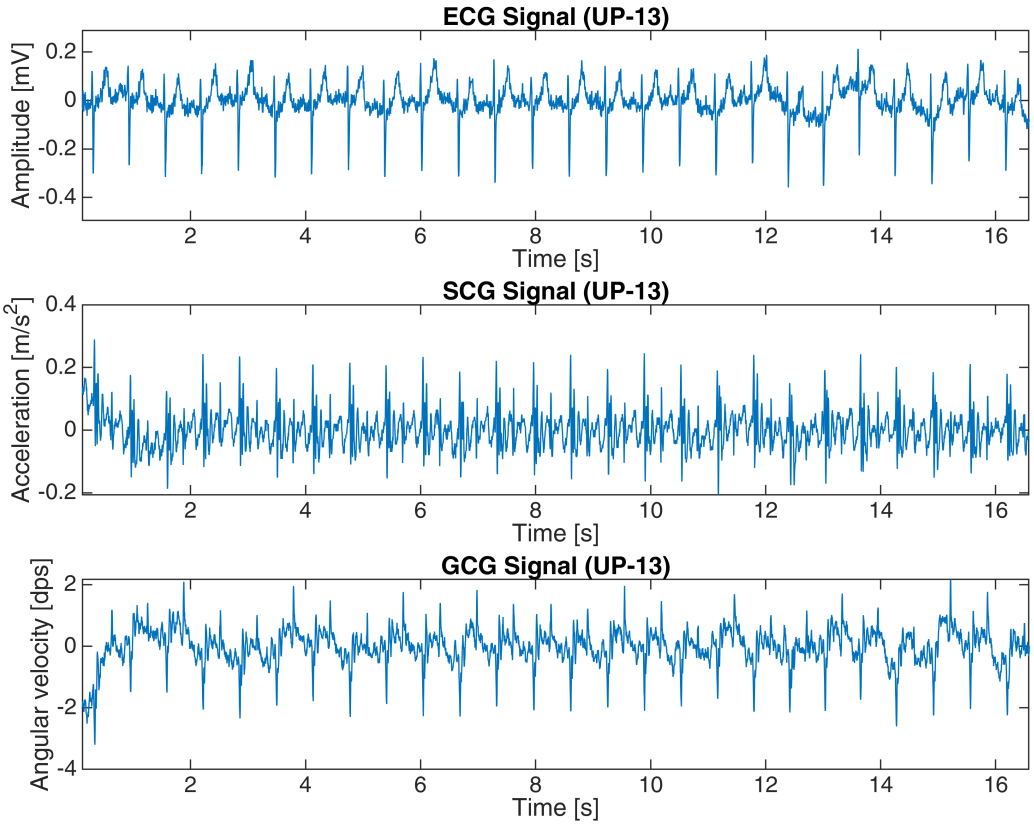

Figure 3. ECG, SCG and GCG signals from subject UP-13 in the second dataset (16-s fragment).

2.2. Signal Processing

Signal processing started with importing the data into MATLAB R2022b (MathWorks, Inc., Natick, MA, USA); data from [67] were directly loaded into the MATLAB workspace, while data from [66] required importing each line of the text files containing signal samples for subjects 1–8 and discarding the first sample (an artifact) for subjects 9–29. In both datasets, each file represented one subject [66,67].

Heartbeat detection in SCG signals and GCG signals for both datasets was based on the approach presented in [11,22,45,53,54,69], which consists of the following steps: The first step was to apply the Pan–Tompkins algorithm (introduced in [70]) to ECG signals. The next step was to find local maxima in the SCG and GCG signals within 100 ms of the closest R waves in the ECG signals based on the observations published in [45,71], and the final step was to calculate the intervals between each consecutive heartbeat in the ECG, SCG and GCG signals [11,69]. An example of a tachogram for a healthy subject is shown in Figure 4, and Figure 5 presents a tachogram of a patient with VHD.

Local maxima that occur within 100 ms of the R wave in concurrent ECG signals are associated with the aortic valve opening waves that are single sharp peaks on the z-axis of the SCG signal and the y-axis of the GCG signal [15,18,20,45,71]. Taking into account only the z-axis of the SCG signal and the y-axis of the GCG signal for analyses was based on the higher signal-to-noise ratio compared to the other axes [15,22,23,65].

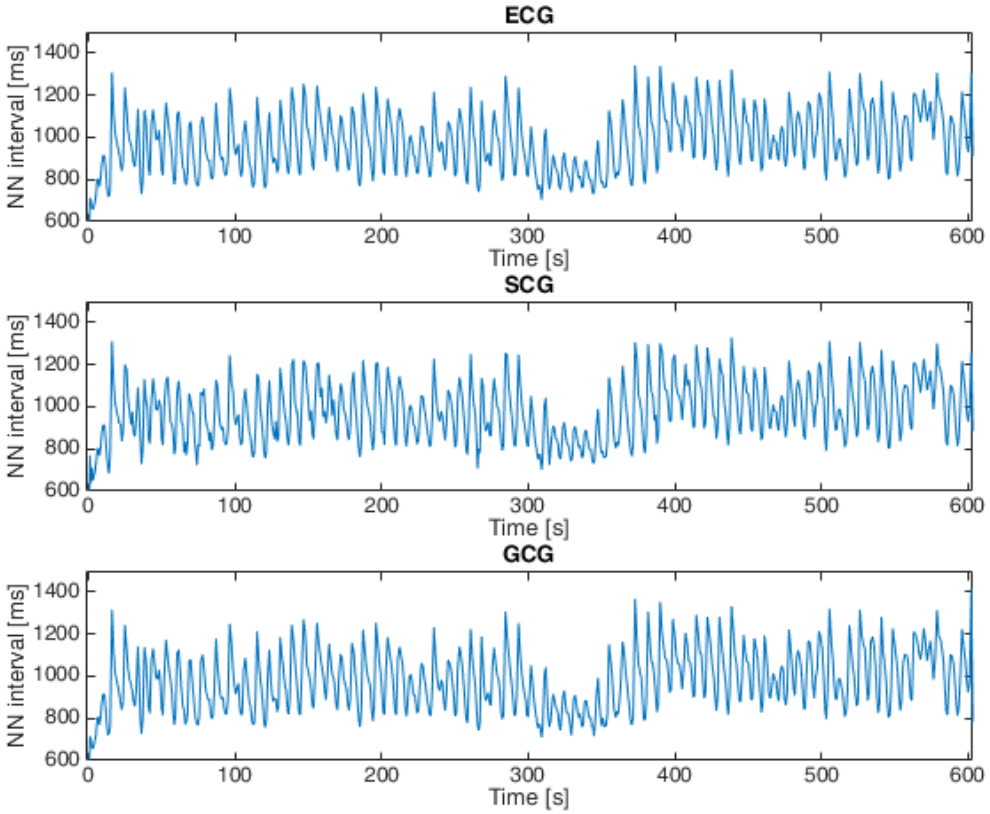

Figure 4. Tachogram derived from ECG, SCG and GCG signals taken from subject 9 in the first dataset (15-second fragment).

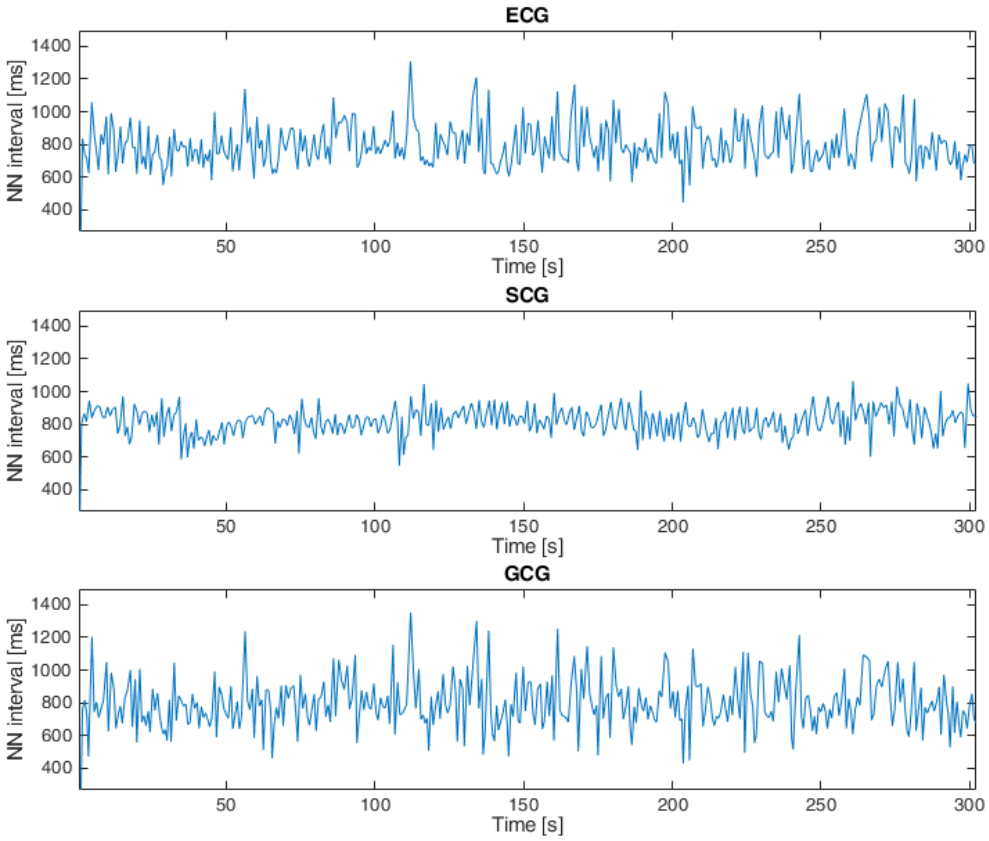

Figure 5. Tachogram ECG, SCG and GCG signals taken from subject UP-09 in the second dataset.

2.3. HRV Analysis

HRV analysis was carried out according to the recommendations published in [56,59] and consisted of the following time and frequency domain indices: mean interbeat interval (AVNN); standard deviation of the interbeat interval (SDNN); root mean square of the differences of successive interbeat intervals (RMSSD); the ratio of successive differences greater than 50 ms in all interbeat intervals (RMSSD); the power of the HRV signal in the very low-frequency band (VLF), in the low-frequency band (LF) and in the high-frequency band (HF); and the LF/HF ratio (LF/HF).

The frequency bands of the HRV spectrum were defined as follows: the very low-frequency band was defined as 0.0033–0.04 Hz, the low frequency band was defined as 0.04–0.15 Hz and the high-frequency band was defined as 0.15–0.4 Hz [56,72]. The analyses were performed with the CardioNet Cardiovascular Signal Toolbox and MATLAB R2022b. HRV indices in the frequency domain were based on spectral power estimates calculated as 1024-sample Lomb periodograms [72,73]. The Lomb periodogram for frequency ω is expressed as:

$$P_x(\omega) = \frac{1}{2}\left(\frac{\left[\sum_j X_j \cos\omega(t_j-\tau)\right]^2}{\sum_j \cos^2\omega(t_j-\tau)} + \frac{\left[\sum_j X_j \sin\omega(t_j-\tau)\right]^2}{\sum_j \sin^2\omega(t_j-\tau)}\right) \quad (1)$$

where τ is the time delay defined in Equation (2), X_j is the value of the j-th sample and t_j is the time of the j-th sample [74,75].

$$\tan 2\omega\tau = \frac{\sum_j \sin 2\omega t_j}{\sum_j \cos 2\omega t_j}. \quad (2)$$

The non-linear analysis of heart rate variability was based on three indices derived from the geometrical features of Poincaré maps: SD_1, SD_2 and SD_1/SD_2.

SD_1 is a measure of the short-term heart rate variability that is defined as the width of an ellipse fitted to scatter points of a Poincaré map and may be expressed as the standard deviation of the distances from the identity line ($y = x$ axis) of the Poincaré plot [76,77]:

$$SD_1 = stddev\left(\frac{|NN_{i+1} - NN_i|}{\sqrt{2}}\right) \quad (3)$$

where NN_i is the i-th inter-beat interval series for $i = 1, 2, \ldots N-1$, NN_{i+1} is the next inter-beat interval and $stddev()$ denotes the standard deviation (SD) [78–81].

SD_2 is the length of an ellipse fitted to the scatter points of a Poincaré map that reflects the long-term heart rate variability and is calculated as the standard deviation of the distance of points from the $y = -x + 2\overline{NN}$ axis:

$$SD_2 = stddev\left(\left|\frac{NN_{i+1} - NN_i}{\sqrt{2}} - 2\overline{NN}\right|\right). \quad (4)$$

SD_1/SD_2 is calculated as the ratio between SD_1 and SD_2 and reflects the unpredictability of the heart rate [82].

3. Results

The results of HRV analyses on electrocardiograms, seismocardiograms and gyrocardiograms obtained from healthy volunteers and patients with VHDs were expressed as the mean and standard deviation (SD) values and are shown in Tables 2–4, respectively. The HRV indices calculated for patients with VHD were derived from [53], except for SD_1, SD_2 and SD_1/SD_2.

The mean and standard deviation values of most HRV indices for patients with VHD are significantly different from those of healthy volunteers, except for AVNN and VLF.

These differences were further evaluated by applying the Student's t-test for the significance level of 0.05. The results of the t-test are shown in Table 5.

Table 2. HRV indices derived from ECG signals from both datasets.

HRV Index	Healthy		VHDs	
	Mean	**SD**	**Mean**	**SD**
AVNN (ms)	952.2551	112.1082	881.7178	155.9992
SDNN (ms)	93.7994	32.0249	94.7063	47.4722
RMSSD (ms)	84.7391	36.1640	121.6602	74.7506
pNN50	0.3092	0.1924	0.3152	0.3178
VLF (ms^2)	2108.3429	1555.0081	960.4883	828.3130
LF (ms^2)	2947.2316	2468.9979	2190.3676	2270.7844
HF (ms^2)	3493.6581	2550.7361	5687.0552	5676.3914
LF/HF	0.9345	0.5333	0.4307	0.1792
SD_1 (ms)	59.9739	26.1703	86.1176	52.9350
SD_2 (ms)	117.6626	39.0786	101.2172	44.6326
SD_1/SD_2	0.5026	0.1258	0.8095	0.2275

Table 3. HRV indices derived from SCG signals from both datasets.

HRV Index	Healthy		VHDs	
	Mean	**SD**	**Mean**	**SD**
AVNN (ms)	952.2583	112.1185	881.5849	156.4511
SDNN (ms)	96.7361	31.9037	113.0716	40.8948
RMSSD (ms)	92.8507	37.1027	160.9644	63.2959
pNN50	0.3590	0.1794	0.5499	0.2345
VLF (ms^2)	2108.0188	1559.9375	1009.8038	849.8141
LF (ms^2)	2967.0571	2477.1760	2413.8259	2320.6393
HF (ms^2)	3898.4718	2926.5900	7275.5874	5670.2440
LF/HF	0.8986	0.5179	0.3177	0.1617
SD_1 (ms)	65.7216	28.4287	113.9518	44.8231
SD_2 (ms)	119.3105	39.8927	110.7745	40.7536
SD_1/SD_2	0.5437	0.1265	1.0515	0.3080

Table 4. HRV indices derived from GCG signals from both datasets.

HRV Index	Healthy		VHDs	
	Mean	**SD**	**Mean**	**SD**
AVNN (ms)	952.2358	113.3623	929.9744	222.8833
SDNN (ms)	86.6979	31.6025	133.0636	66.8667
RMSSD (ms)	83.6785	36.3714	183.8181	79.3316
pNN50	0.3712	0.1717	0.5551	0.2799
VLF (ms^2)	2119.8767	1568.1258	3880.6816	13,313.9379
LF (ms^2)	2978.3266	2484.0123	3251.1583	3594.0590
HF (ms^2)	3663.0536	2657.3141	9481.6615	7681.8666
LF/HF	0.8997	0.5328	0.3217	0.1611
SD_1 (ms)	63.7232	26.2834	130.1497	56.1906
SD_2 (ms)	118.6764	39.0182	130.1935	80.8863
SD_1/SD_2	0.5347	0.1369	1.0302	0.2766

The differences between the HRV indices in healthy volunteers and in patients with VHD shown in Table 5 are statistically significant for all analyzed HRV indices except for AVNN, SDNN, pNN50 (ECG), VLF (GCG), LF and SD_2. This proves a significant influence of ventricular heart diseases on the results of heart rate variability in time domain, frequency domain and nonlinear analyses. These results confirm the findings related to Table 3.

Table 5. Results of Student's *t*-tests between healthy subjects and VHD subjects.

HRV Index	ECG		SCG		GCG	
	h *	*p*-Value	h *	*p*-Value	h *	*p*-Value
AVNN	0	0.0516	0	0.0516	0	0.6316
SDNN	0	0.9320	0	0.0748	1	0.0085
RMSSD	1	0.0201	1	<0.0001	1	<0.0001
pNN50	0	0.8544	1	<0.0001	1	<0.0001
VLF	1	<0.0001	1	0.0012	0	0.4823
LF	0	0.5215	0	0.3742	0	0.7365
HF	0	0.0621	1	0.0028	1	<0.0001
LF/HF	1	<0.0001	1	<0.0001	1	<0.0001
SD_1	1	0.0201	1	<0.0001	1	<0.0001
SD_2	0	0.4502	0	0.6924	0	0.3863
SD_1/SD_2	1	<0.0001	1	<0.0001	1	<0.0001

* h = 0 means no significant difference.

The findings reported in [17,22,45,51] for HRV indices obtained from ECG, SCG and GCG signals in healthy volunteers and patients with VHDs were verified with the Pearson's linear correlation that were expressed as Pearson's linear correlation coefficient (ρ) for healthy volunteers and VHD patients. A linear correlation coefficient larger than 0.7 was considered as a strong linear correlation between two given datasets [83].

The results presented in Table 6 indicate a strong linear correlation for the *p*-value under 0.001, except for SD_1/SD_2 between ECG and SCG signals from VHD patients. The correlation between the analyzed HRV indices obtained from ECG and GCG signals (as shown in Table 7) is weaker than between the ECG and SCG signals, but remains strong for all HRV indices except for VLF, SD_2 and SD_1/SD_2. The strongest correlation is observed for HF, pNN50, RMSSD and SD_1, and the weakest correlation is observed for VLF (−0.0663).

Table 6. Pearson's linear correlation coefficient of HRV indices obtained from ECG and SCG signals.

HRV Index	ρ (Healthy Subjects)	ρ (VHD Subjects)
AVNN	1.0000	0.9999
SDNN	0.9942	0.8767
RMSSD	0.9754	0.8164
pNN50	0.6402	0.7026
VLF	0.9999	0.8867
LF	0.9996	0.9390
HF	0.9868	0.9493
LF/HF	0.9916	0.7296
SD_1	0.9754	0.8164
SD_2	0.9980	0.9364
SD_1/SD_2	0.9375	0.4116

Table 7. Pearson's linear correlation coefficient of HRV indices obtained from ECG and GCG signals.

HRV Index	ρ (Healthy Subjects)	ρ (VHD Subjects)
AVNN	1.0000	0.5602
SDNN	0.9942	0.4830
RMSSD	0.9754	0.6134
pNN50	0.6402	0.6497
VLF	0.9999	−0.0663
LF	0.9996	0.5105
HF	0.9842	0.6818
LF/HF	0.9906	0.6531
SD_1	0.9976	0.6132
SD_2	0.9998	0.3829
SD_1/SD_2	0.9841	0.3684

4. Discussion

We have performed HRV analysis on electrocardiograms, seismocardiograms and gyrocardiograms from healthy volunteers and patients with VHD based on publicly available datasets.

The mean and standard deviation values of HRV indices obtained from healthy subjects are similar to those reported by Siecinski et al. in [22,50,52,53], except for the LF/HF and frequency domain indices in [22,52], and also similar to the results reported by Ramos-Castro et al. in [43] and Tadi et al. in [45]. The discrepancies in the mean HRV indices are within the standard deviation for each signal (ECG, SCG and GCG) and may be related to inter-subject variations.

The mean and standard deviation values of most HRV indices for patients with VHD are significantly different from those of healthy volunteers, except for AVNN, LF and SD_2. This observation was confirmed by a Student's t-test. Despite the fact that RMSSD and SD_1 should be identical [76], there were significant differences between these indices in each case.

We have shown the significant influence of valvular heart disease on HRV indices, except for AVNN, SDNN (ECG and SCG), pNN50 (ECG), VLF (GCG), LF, HF (ECG) and SD_2, which was in line with [84,85]. The similarities between the results of the HRV analysis in patients with VHD in our study and those reported in [84] prove that the HRV indices obtained from seismocardiograms are valid both for healthy subjects, patients with aortic stenosis and also for other VHD patients as long as heartbeats were reliably detected [45,53,54,62].

Despite the significant influence of VHDs on HRV indices, the correlation between the HRV indices obtained from ECG and SCG signals is strong, except for SD_2. Obtained values of ρ are similar to those reported by Siecinski et al. in [50] and Charlier et al. in [86]. However, the correlations of analyzed pairs of signals are weaker for VHD patients than for healthy volunteers, especially the correlations of HRV indices from ECG and GCG signals [22,43,45,52].

Such results are influenced by age (the population of healthy volunteers is significantly younger than those of patients with VHD), comorbidities, signal quality and the use of different accelerometers and gyroscopes operating with different sampling frequency and accuracy, according to the available datasheets [68,87,88].

The differences between RMSSD and SD_1 values did not result in significantly different ρ values. This indicates the lower accuracy of automatic heartbeat detection in SCG and GCG signals of patients with VHDs that was affected by morphological changes caused by VHDs and/or ageing [53,54].

The limitations of the study include the use of only one type of heartbeat detector for seismocardiograms and gyrocardiograms that depends on a concurrent electrocardiogram, the influence of specific cardiovascular conditions or medication on the calculated HRV indices was not considered and the morphological changes in SCG and GCG signals due to valvular heart disease was not evaluated.

In future studies, we will consider evaluating the influence of various cardiovascular conditions on HRV indices derived from ECG, SCG and GCG signals; indices derived from larger and more diverse groups, including the analysis of SCG and GCG signal morphology; and indices derived from other detectors of SCG and GCG signals. In this study, we proved that a heart rate variability analysis based on cardiac mechanical signals [30,31,89] may be useful for a more cost-effective and convenient diagnosis and monitoring of patients with cardiovascular disease.

5. Conclusions

The results of the heart rate variability analysis based on mechanocardiograms (SCG and GCG signals) in both a healthy population and patients with VHD remain valid as long as heartbeats are correctly detected. Valvular heart disease significantly affects RMSSD, pNN50 (only SCG and GCG signals), VLF (only ECG and SCG signals), HF (only SCG and

GCG signals), LF/HF, SD_1 and SD_1/SD_2. The linear correlation between the HRV indices obtained from the ECG and the mechanocardiograms is strong both in healthy volunteers and in patients with VHD, except for SD_2.

Future studies should include an evaluation of other cardiovascular conditions, larger and more diverse groups and other heartbeat detection methods for mechanocardiograms, and an analysis of the morphology of cardiac mechanical signals. We showed that mechanocardiogram-based heart rate variability analyses can be used in the diagnosis and monitoring of cardiovascular disease, which could be more cost-effective and convenient for patients.

Supplementary Materials: The following supporting information can be downloaded at: https://www.mdpi.com/article/10.3390/s23042152/s1.

Author Contributions: Conceptualization, S.S.; methodology, S.S.; software, S.S.; validation, S.S. and P.S.K.; formal analysis, S.S.; investigation, S.S.; resources, S.S.; data curation, S.S.; writing—original draft preparation, S.S.; writing—review and editing, S.S., E.J.T. and P.S.K.; visualization, S.S.; supervision, E.J.T. and P.S.K.; project administration, E.J.T. and P.S.K.; funding acquisition, E.J.T. All authors have read and agreed to the published version of the manuscript.

Funding: This research received no external funding.

Institutional Review Board Statement: Not applicable.

Informed Consent Statement: Not applicable.

Data Availability Statement: The research was based on publicly available data published in [66,67]. Supplementary data (source code and full results) are available online. However, the data presented in this study are available on request from the corresponding author.

Conflicts of Interest: The authors declare no conflict of interest.

Abbreviations

The following abbreviations are used in this manuscript:

VHD	Valvular heart disease
HRV	Heart rate variability
ECG	Electrocardiography, electrocardiogram
SCG	Seismocardiography
GCG	Gyrocardiography
MEMS	Microelectromechanical systems
MRI	Magnetic resonance imaging
EMD	Empirical mode decomposition
CABG	Coronary artery bypass graft surgery
F	Female
MR	Mitral valve regurgitation
MS	Mitral valve stenosis
M	Male
MI	Myocardial infarction
NN	The interval between consecutive normal heartbeats
FIR	Fininte impulse response (filter)
AO	Aortic valve opening (wave)
RSA	Respiratory sinus arrhythmia
SNR	Signal-to-noise (ratio)
AVNN	Mean inter-beat interval
SDNN	Standard deviation of all interbeat intervals
RMSSD	Root mean square of differences (RMSSD) of successive inter-beat intervals
pNN50	The proportion of the number of pairs of successive differences greater than 50 ms divided by total number of normal inter-beat intervals

VLF	The power of very low frequency band (0.0033–0.04 Hz) of HRV spectrum
LF	The power of low frequency band (0.04–0.15 Hz) of HRV spectrum
HF	The power of high frequency band (0.15–0.4 Hz) of HRV spectrum
LF/HF	LF/HF ratio
SD_1	The width of the ellipse which containes the scatter points of Poincaré map
SD_2	The length of the ellipse which containes the scatter points of Poincaré map
SD_1/SD_2	SD_1 to SD_2 ratio
AVD	Aortic valve disease
AC	Aortic valve closure
AO	Aortic valve opening
MC	Mitral valve closure
MO	Mitral valve opening
PCI	Percutaneous coronary intervention
AS	Aortic valve stenosis
AR	Aortic valve regurgitation
TR	Tricupsid valve regurgitation
ρ	Pearson's linear correlation coefficient

Appendix A. Recording Descriptions in Datasets

This appendix presents a complete description of the recordings in both analyzed datasets based on available metadata [66,67]; the recordings from the healthy volunteers dataset (Mechanocardiograms with ECG reference) are shown in Table A1, while the full description of the recordings in the VHD patients dataset is presented in Table A2.

Table A1. Recording description in the "Mechanocardiograms with ECG reference" dataset.

Subject	Length of Recording	Position	Breathing	Remarks
1	3 min	Left or right side	2 min normal, 30 s holding a breath, 30 s normal	
2	3 min	Left or right side	2 min normal, 30 s holding a breath, 30 s normal	
3	3 min	Left or right side	2 min normal, 30 s holding a breath, 30 s normal	
4	3 min	Left or right side	2 min normal, 30 s holding a breath, 30 s normal	
5	3 min	Left or right side	2 min normal, 30 s holding a breath, 30 s normal	
6	3 min	Left or right side	2 min normal, 30 s holding a breath, 30 s normal	Sensor not strictly secured on chest because of body hair.
7	3 min	Left or right side	2 min normal, 30 s holding a breath, 30 s normal	
8	3 min	Supine	Normal	
9	10 min	Supine	Normal	
10	10 min	Supine	Normal	
11	30 min	Supine	Normal	
12	10 min	Supine	Normal	
13	10 min	Supine	Normal	

Table A1. *Cont.*

Subject	Length of Recording	Position	Breathing	Remarks
14	10 min	Supine	Normal	
15	10 min	Supine	Normal	
16	10 min	Supine	Normal	
17	10 min	Supine	Normal	
18	10 min	Supine	Normal	
19	10 min	Supine	Normal	
20	10 min	Supine	Normal	
21	10 min	Supine	Normal	
22	10 min	Supine	Normal	Sensor loose in the end.
23	10 min	Left or right side	Normal	
24	10 min	Supine	Normal	
25	9 min	Supine	Normal	
26	10 min	Supine	Normal	
27	10 min	Left or right side	Normal	
28	10 min	Supine	Normal	
29	10 min	Supine	Normal	

Table A2. Recording description in "An Open-access Database for the Evaluation of Cardio-mechanical Signals from Patients with Valvular Heart Diseases" dataset.

Subject Number	Length of Recording	Age (years)	Gender	Height (cm)	Weight (kg)	History of			MS	MR	AR	AS	TR
						MI	CABG	PCI					
UP-01	6 min 8 s	89	M	154.9	49.0	0	1	1	0	0	0	1	1
UP-02	6 min 10 s	89	M	170.2	82.0	1	1	1	0	0	0	1	0
UP-03	6 min 1 s	96	M	162.5	66.0	0	1	1	0	0	0	1	1
UP-04	5 min 36 s	84	M	152.4	65.0	0	1	1	0	0	0	1	0
UP-05	6 min 35 s	70	F	162.5	79.0	0	1	1	0	0	0	1	1
UP-06	5 min 39 s	90	F	160	48.0	1	1	1	0	0	0	1	1
UP-07	6 min 3 s	84	M	162.5	79.0	0	1	1	0	0	0	1	0
UP-08	5 min 11 s	95	F	152.4	44.0	0	1	1	1	0	0	1	1
UP-09	5 min 15 s	89	M	182.8	90.7	0	1	1	0	0	0	1	0
UP-10	5 min 2 s	80	F	157.4	74.0	0	1	1	1	0	0	1	0
UP-11	5 min 6 s	68	M	177.8	79.0	0	1	1	0	0	0	1	0
UP-12	5 min 10 s	79	F	154.9	78.0	0	1	1	1	0	0	1	0
UP-13	5 min 18 s	95	F	160	73.0	0	1	1	0	1	0	1	0
UP-14	5 min 38 s	85	F	152	82.0	0	1	1	1	0	0	1	0
UP-15	5 min 34 s	84	F	175	76.0	0	1	1	0	0	0	1	0
UP-16	5 min 44 s	97	M	157	77.0	0	1	1	0	0	0	1	0
UP-17	5 min 54 s	80	M	182.8	86.0	0	1	1	0	0	0	1	1
UP-18	5 min 9 s	90	F	152.4	92.0	0	1	1	0	0	0	1	0
UP-19	5 min 17 s	78	M	170.1	78.0	0	1	1	0	0	0	1	0
UP-20	7 min 49 s	92	F	139.7	53.0	0	1	1	0	1	0	1	0
UP-21	5 min 10 s	72	M	172.7	68.0	0	1	1	1	1	0	1	1
UP-22	10 min 3 s	77	F	165.1	51.3	0	0	0	0	0	0	1	1
UP-23	9 min 59 s	84	F	139.7	70.3	0	0	0	0	0	0	1	0
UP-24	5 min	80	F	155	67.6	0	0	0	0	0	0	1	1
UP-25	9 min 5 s	87	F	155.0	54.0	0	0	0	0	1	0	1	0
UP-26	5 min 8 s	80	M	175.3	85.7	0	0	1	0	0	0	1	0
UP-27	5 min 5 s	82	M	180.0	118.0	0	0	0	0	0	0	1	0
UP-28	5 min 2 s	71	M	175.0	117.0	0	0	0	0	0	0	1	0
UP-29	4 min 58 s	80	M	168.9	65.8	0	0	0	1	0	0	1	0
UP-30	4 min 59 s	71	M	177.8	81.6	0	0	1	1	0	0	1	0

M: male; F: female; MI: myocardial infarction; CABG: coronary artery bypass graft surgery; PCI: percutaneous coronary intervention; MS: mitral valve stenosis; MR: mitral valve regurgitation; AS: aortic valve stenosis; AR: aortic valve regurgitation; TR: tricupsid valve regurgitation; The presence of the cardiac condition: 1—yes; 0—no.

References

1. Mensah, G.A.; Roth, G.A.; Fuster, V. The Global Burden of Cardiovascular Diseases and Risk Factors: 2020 and Beyond. *J. Am. Coll. Cardiol.* **2019**, *74*, 2529–2532.[CrossRef]
2. World Health Organization. *Global Action Plan for the Prevention and Control of Noncommunicable Diseases 2013–2020*; World Health Organization: Geneva, Switzerland, 2013.
3. World Health Organization. The Top 10 Causes of Death. 2020. Available online: https://www.who.int/news-room/fact-sheets/detail/the-top-10-causes-of-death (accessed on 3 February 2023).
4. World Health Organization. *World Health Statistics 2020: Monitoring Health for the SDGs, Sustainable Development Goals*; World Health Organization: Geneva, Switzerland, 2020; 77p.
5. Virani, S.S.; Alonso, A.; Aparicio, H.J.; Benjamin, E.J.; Bittencourt, M.S.; Callaway, C.W.; Carson, A.P.; Chamberlain, A.M.; Cheng, S.; Delling, F.N.; et al. Heart Disease and Stroke Statistics—2021 Update. *Circulation* **2021**, *143*, e254–e743. [CrossRef]
6. Coffey, S.; Roberts-Thomson, R.; Brown, A.; Carapetis, J.; Chen, M.; Enriquez-Sarano, M.; Zühlke, L.; Prendergast, B.D. Global epidemiology of valvular heart disease. *Nat. Rev. Cardiol.* **2021**, *18*, 853–864. [CrossRef]
7. Nkomo, V.T.; Gardin, J.M.; Skelton, T.N.; Gottdiener, J.S.; Scott, C.G.; Enriquez-Sarano, M. Burden of valvular heart diseases: A population-based study. *Lancet* **2006**, *368*, 1005–1011. [CrossRef]
8. Maganti, K.; Rigolin, V.H.; Sarano, M.E.; Bonow, R.O. Valvular Heart Disease: Diagnosis and Management. *Mayo Clin. Proc.* **2010**, *85*, 483–500. [CrossRef]
9. Vahanian, A.; Beyersdorf, F.; Praz, F.; Milojevic, M.; Baldus, S.; Bauersachs, J.; Capodanno, D.; Conradi, L.; De Bonis, M.; De Paulis, R.; et al. 2021 ESC/EACTS Guidelines for the management of valvular heart disease: Developed by the Task Force for the management of valvular heart disease of the European Society of Cardiology (ESC) and the European Association for Cardio-Thoracic Surgery (EACTS). *Eur. Heart J.* **2022**, 43, 561–632. [CrossRef]
10. Yang, Y.; Wang, Z.; Chen, Z.; Wang, X.; Zhang, L.; Li, S.; Zheng, C.; Kang, Y.; Jiang, L.; Zhu, Z.; et al. Current status and etiology of valvular heart disease in China: A population-based survey. *BMC Cardiovasc. Disord.* **2021**, *21*, 339. [CrossRef]
11. Yang, C.; Fan, F.; Aranoff, N.; Green, P.; Li, Y.; Liu, C.; Tavassolian, N. An Open-Access Database for the Evaluation of Cardio-Mechanical Signals From Patients with Valvular Heart Diseases. *Front. Physiol.* **2021**, *12*, 750221. [CrossRef]
12. Alugubelli, N.; Abuissa, H.; Roka, A. Wearable Devices for Remote Monitoring of Heart Rate and Heart Rate Variability—What We Know and What Is Coming. *Sensors* **2022**, *22*, 8903. [CrossRef]
13. Taoum, A.; Bisiaux, A.; Tilquin, F.; Le Guillou, Y.; Carrault, G. Validity of Ultra-Short-Term HRV Analysis Using PPG—A Preliminary Study. *Sensors* **2022**, *22*, 7995. [CrossRef]
14. Glaveckaite, S.; Petrikonyte, D.; Latveniene, L.; Serpytis, P.; Laucevicius, A. Ocena choroby zastawkowej serca za pomocą elektrokardiografii wysiłkowej i echokardiografii obciążeniowej: Czy te badania są nadal potrzebne? *Folia Cardiol.* **2018**, *13*, 318–330. [CrossRef]
15. Tadi, M.J.; Lehtonen, E.; Saraste, A.; Tuominen, J.; Koskinen, J.; Teräs, M.; Airaksinen, J.; Pänkäälä, M.; Koivisto, T. Gyrocardiography: A New Non-invasive Monitoring Method for the Assessment of Cardiac Mechanics and the Estimation of Hemodynamic Variables. *Sci. Rep.* **2017**, *7*, 6823. [CrossRef] [PubMed]
16. Rai, D.; Thakkar, H.K.; Rajput, S.S.; Santamaria, J.; Bhatt, C.; Roca, F. A Comprehensive Review on Seismocardiogram: Current Advancements on Acquisition, Annotation, and Applications. *Mathematics* **2021**, *9*, 2243. [CrossRef]
17. Tadi, M.J.; Lehtonen, E.; Pankäälä, M.; Saraste, A.; Vasankari, T.; Terás, M.; Koivisto, T. Gyrocardiography: A new non-invasive approach in the study of mechanical motions of the heart. Concept, method and initial observations. In Proceedings of the 2016 38th Annual International Conference of the IEEE Engineering in Medicine and Biology Society (EMBC), Orlando, FL, USA, 16–20 August 2016; pp. 2034–2037. [CrossRef]
18. Sieciński, S.; Kostka, P.S.; Tkacz, E.J. Gyrocardiography: A Review of the Definition, History, Waveform Description, and Applications. *Sensors* **2020**, *20*, 6675. [CrossRef] [PubMed]
19. Bozhenko, B. Seismocardiography—A new method in the study of the functional condition of the heart. *Ter. Arkhiv* **1961**, *33*, 55–64.
20. Zanetti, J.M.; Salerno, D.M. Seismocardiography: A technique for recording precordial acceleration. In Proceedings of the [1991] Computer-Based Medical Systems, Proceedings of the Fourth Annual IEEE Symposium, Baltimore, MD, USA, 12–14 May 1991; pp. 4–9. [CrossRef]
21. Meriheinä, U.; Juppo, M.; Koivisto, T.; Mikko, P.; Sairanen, K.; Grönholm, M. Heart Monitoring System. WIPO Patent WO 2015/036925 A1, 19 March 2015.
22. Sieciński, S.; Kostka, P.S.; Tkacz, E.J. Heart Rate Variability Analysis on Electrocardiograms, Seismocardiograms and Gyrocardiograms on Healthy Volunteers. *Sensors* **2020**, *20*, 4522. [CrossRef]
23. Zanetti, J.M.; Tavakolian, K. Seismocardiography: Past, present and future. In Proceedings of the 2013 35th Annual International Conference of the IEEE Engineering in Medicine and Biology Society (EMBC), Osaka, Japan, 3–7 July 2013; pp. 7004–7007. [CrossRef]
24. Inan, O.T.; Migeotte, P.F.; Park, K.S.; Etemadi, M.; Tavakolian, K.; Casanella, R.; Zanetti, J.; Tank, J.; Funtova, I.; Prisk, G.K.; et al. Ballistocardiography and Seismocardiography: A Review of Recent Advances. *IEEE J. Biomed. Health Inform.* **2015**, *19*, 1414–1427. [CrossRef]

25. Gurev, V.; Tavakolian, K.; Constantino, J.C.; Kaminska, B.; Blaber, A.P.; Trayanova, N. Mechanisms underlying isovolumic contraction and ejection peaks in seismocardiogram morphology. *J. Med. Biol. Eng.* **2012**, *32*, 103. [CrossRef]
26. Dehkordi, P.; Khosrow-Khavar, F.; Di Rienzo, M.; Inan, O.T.; Schmidt, S.E.; Blaber, A.P.; Sørensen, K.; Struijk, J.J.; Zakeri, V.; Lombardi, P.; et al. Comparison of Different Methods for Estimating Cardiac Timings: A Comprehensive Multimodal Echocardiography Investigation. *Front. Physiol.* **2019**, *10*, 1057. [CrossRef]
27. Santucci, F.; Lo Presti, D.; Massaroni, C.; Schena, E.; Setola, R. Precordial Vibrations: A Review of Wearable Systems, Signal Processing Techniques, and Main Applications. *Sensors* **2022**, *22*, 5805. [CrossRef]
28. Wajdan, A.; Jahren, T.S.; Villegas-Martinez, M.; Khan, F.H.; Halvorsen, P.S.; Odland, H.H.; Elle, O.J.; Solberg, A.H.S.; Remme, E.W. Automatic Detection of Aortic Valve Events Using Deep Neural Networks on Cardiac Signals From Epicardially Placed Accelerometer. *IEEE J. Biomed. Health Inform.* **2022**, *26*, 4450–4461. [CrossRef]
29. Taebi, A.; Solar, B.E.; Bomar, A.J.; Sandler, R.H.; Mansy, H.A. Recent Advances in Seismocardiography. *Vibration* **2019**, *2*, 64–86. [CrossRef]
30. Yang, C.; Ojha, B.D.; Aranoff, N.D.; Green, P.; Tavassolian, N. Classification of aortic stenosis using conventional machine learning and deep learning methods based on multi-dimensional cardio-mechanical signals. *Sci. Rep.* **2020**, *10*, 17521. [CrossRef]
31. Shokouhmand, A.; Aranoff, N.D.; Driggin, E.; Green, P.; Tavassolian, N. Efficient detection of aortic stenosis using morphological characteristics of cardiomechanical signals and heart rate variability parameters. *Sci. Rep.* **2021**, *11*, 23817. [CrossRef]
32. Johnson, E.M.; Robinson, J.D.; Rigsby, C.K.; McCarthy, P.M.; Malaisrie, S.C.; Allen, B.D.; Barker, A.J.; Markl, M. Abstract 9903: Artificial Intelligence Driven Wearable 2-minute Seismocardiography Test for Detection of Aortic Valve Stenosis Severity. *Circulation* **2022**, *146*, A9903–A9903. ._1.9903. [CrossRef]
33. Johnson, E.M.; Barker, A.J.; Robinson, J.D.; Rigsby, C.K.; Markl, M. Abstract 11504: Elevated Seismocardiography-Derived Chest Energy is Associated With Aortic Flow Abnormalities in Patients With Aortic Valve Disease. *Circulation* **2022**, *146*, A11504. ._1.11504. [CrossRef]
34. Korzeniowska-Kubacka, I.; Bilinska, M.; Piotrowicz, R. Usefulness of Seismocardiography for the Diagnosis of Ischemia in Patients with Coronary Artery Disease. *Ann. Noninvasive Electrocardiol.* **2005**, *10*, 281–287. [CrossRef]
35. Iftikhar, Z.; Lahdenoja, O.; Tadi, M.J.; Hurnanen, T.; Vasankari, T.; Kiviniemi, T.; Airaksinen, J.; Koivisto, T.; Pänkäälä, M. Multiclass Classifier based Cardiovascular Condition Detection Using Smartphone Mechanocardiography. *Sci. Rep.* **2018**, *8*, 9344. [CrossRef]
36. Mehrang, S.; Jafari Tadi, M.; Kaisti, M.; Lahdenoja, O.; Vasankari, T.; Kiviniemi, T.; Airaksinen, J.; Koivisto, T.; Pänkäälä, M. Machine Learning Based Classification of Myocardial Infarction Conditions Using Smartphone-Derived Seismo- and Gyrocardiography. In Proceedings of the 2018 Computing in Cardiology Conference (CinC), Maastricht, The Netherlands, 23–26 September 2018; Volume 45, pp. 1–4. [CrossRef]
37. Hurnanen, T.; Lehtonen, E.; Tadi, M.J.; Kuusela, T.; Kiviniemi, T.; Saraste, A.; Vasankari, T.; Airaksinen, J.; Koivisto, T.; Pankaala, M. Automated Detection of Atrial Fibrillation Based on Time–Frequency Analysis of Seismocardiograms. *IEEE J. Biomed. Health Inform.* **2017**, *21*, 1233–1241. [CrossRef]
38. Jafari Tadi, M.; Mehrang, S.; Kaisti, M.; Lahdenoja, O.; Hurnanen, T.; Jaakkola, J.; Jaakkola, S.; Vasankari, T.; Kiviniemi, T.; Airaksinen, J.; et al. Comprehensive Analysis of Cardiogenic Vibrations for Automated Detection of Atrial Fibrillation Using Smartphone Mechanocardiograms. *IEEE Sens. J.* **2019**, *19*, 2230–2242. [CrossRef]
39. Mehrang, S.; Tadi, M.J.; Hurnanen, T.; Knuutila, T.; Lahdenoja, O.; Jaakkola, J.; Jaakkola, S.; Vasankari, T.; Kiviniemi, T.; Airaksinen, J.; et al. Reliability of Self-Applied Smartphone Mechanocardiography for Atrial Fibrillation Detection. *IEEE Access* **2019**, *7*, 146801–146812. [CrossRef]
40. Mehrang, S.; Tadi, M.J.; Knuutila, T.; Jaakkola, J.; Jaakkola, S.; Kiviniemi, T.; Vasankari, T.; Airaksinen, J.; Koivisto, T.; Pänkäälä, M. End-to-end sensor fusion and classification of atrial fibrillation using deep neural networks and smartphone mechanocardiography. *Physiol. Meas.* **2022**, *43*, 055004. [CrossRef] [PubMed]
41. Sørensen, K.; Søgaard, P.; Emerek, K.; Jensen, A.S.; Struijk, J.J.; Schmidt, S.E. Seismocardiography as a tool for assessment of bi-ventricular pacing. *Physiol. Meas.* **2022**, *43*, 105007. [CrossRef] [PubMed]
42. Koivisto, T.; Lahdenoja, O.; Hurnanen, T.; Koskinen, J.; Jafarian, K.; Vasankari, T.; Jaakkola, S.; Kiviniemi, T.O.; Airaksinen, K.E.J. Mechanocardiography-Based Measurement System Indicating Changes in Heart Failure Patients during Hospital Admission and Discharge. *Sensors* **2022**, *22*, 9781. [CrossRef]
43. Ramos-Castro, J.; Moreno, J.; Miranda-Vidal, H.; García-González, M.A.; Fernández-Chimeno, M.; Rodas, G.; Capdevila, L. Heart rate variability analysis using a seismocardiogram signal. In Proceedings of the 2012 Annual International Conference of the IEEE Engineering in Medicine and Biology Society, San Diego, CA, USA, 28 August–1 September 2012; pp. 5642–5645. [CrossRef]
44. Choudhary, T.; Das, M.; Sharma, L.; Bhuyan, M. Analyzing seismocardiographic approach for heart rate variability measurement. *Biomed. Signal Process. Control* **2021**, *68*, 102793. [CrossRef]
45. Tadi, M.J.; Lehtonen, E.; Koivisto, T.; Pänkäälä, M.; Paasio, A.; Teräs, M. Seismocardiography: Toward heart rate variability (HRV) estimation. In Proceedings of the 2015 IEEE International Symposium on Medical Measurements and Applications (MeMeA) Proceedings, Turin, Italy, 7–9 May 2015; pp. 261–266. [CrossRef]
46. Landreani, F.; Morri, M.; Martin-Yebra, A.; Casellato, C.; Pavan, E.; Frigo, C.; Caiani, E.G. Ultra-short-term heart rate variability analysis on accelerometric signals from mobile phone. In Proceedings of the 2017 E-Health and Bioengineering Conference (EHB), Sinaia, Romania, 22–24 June 2017; pp. 241–244. [CrossRef]

47. Landreani, F.; Faini, A.; Martin-Yebra, A.; Morri, M.; Parati, G.; Caiani, E.G. Assessment of Ultra-Short Heart Variability Indices Derived by Smartphone Accelerometers for Stress Detection. *Sensors* **2019**, *19*, 3729. [CrossRef]
48. Londhe, A.N.; Atulkar, M. Heart Rate Variability: A Methodological Survey. In Proceedings of the 2019 International Conference on Intelligent Sustainable Systems (ICISS), Palladam, India, 21–22 February 2019; pp. 57–63. [CrossRef]
49. Shokouhmand, A.; Yang, C.; Aranoff, N.D.; Driggin, E.; Green, P.; Tavassolian, N. Mean Pressure Gradient Prediction Based on Chest Angular Movements and Heart Rate Variability Parameters. In Proceedings of the 2021 43rd Annual International Conference of the IEEE Engineering in Medicine Biology Society (EMBC), Guadalajara, Mexico, 1–5 November 2021; pp. 7170–7173. [CrossRef]
50. Siecinski, S.; Kostka, P.S.; Tkacz, E.J. Heart Rate Variability Analysis on CEBS Database Signals. In Proceedings of the 2018 40th Annual International Conference of the IEEE Engineering in Medicine and Biology Society, Honolulu, HI, USA, 18–21 July 2018; pp. 5697–5700. [CrossRef]
51. Siecinski, S.; Tkacz, E.J.; Kostka, P.S. Comparison of HRV indices obtained from ECG and SCG signals from CEBS database. *BioMedical Eng. OnLine* **2019**, *18*, 69. [CrossRef]
52. Siecinski, S.; Kostka, P.S.; Tkacz, E.J. Time Domain Furthermore, Frequency Domain Heart Rate Variability Analysis on Gyrocardiograms. In Proceedings of the 2020 42nd Annual International Conference of the IEEE Engineering in Medicine and Biology Society (EMBC), Montreal, QC, Canada, 20–24 July 2020; pp. 2630–2633. [CrossRef]
53. Siecinski, S.; Kostka, P.S.; Tkacz, E.J. Time Domain and Frequency Domain Heart Rate Variability Analysis on Electrocardiograms and Mechanocardiograms from Patients with Valvular Diseases. In Proceedings of the 2022 44th Annual International Conference of the IEEE Engineering in Medicine and Biology Society (EMBC), Glasgow, UK, 11–15 July 2022; pp. 653–656. [CrossRef]
54. Siecinski, S.; Kostka, P.S.; Tkacz, E.J. Comparison of Heart Rate Variability Indices Based on Seismocardiograms from Healthy Volunteers and Patients with Valvular Heart Diseases. In Proceedings of the Computing in Cardiology Conference, Tampere, Finland, 4–7 September 2022.
55. Milena, v.; Romano, C.; De Tommasi, F.; Carassiti, M.; Formica, D.; Schena, E.; Massaroni, C. Linear and Non-Linear Heart Rate Variability Indexes from Heart-Induced Mechanical Signals Recorded with a Skin-Interfaced IMU. *Sensors* **2023**, *23*, 1615. [CrossRef]
56. Task Force of the European Society of Cardiology the North American Society of Pacing Electrophysiology . Heart Rate Variability. Standards of Measurement, Physiological Interpretation, and Clinical Use. *Circulation* **1996**, *93*, 1043–1065. [CrossRef]
57. Saykrs, B. Analysis of Heart Rate Variability. *Ergonomics* **1973**, *16*, 17–32. . [CrossRef]
58. Montano, N.; Porta, A.; Cogliati, C.; Costantino, G.; Tobaldini, E.; Casali, K.R.; Iellamo, F. Heart rate variability explored in the frequency domain: A tool to investigate the link between heart and behavior. *Neurosci. Biobehav. Rev.* **2009**, *33*, 71–80. [CrossRef]
59. Sassi, R.; Cerutti, S.; Lombardi, F.; Malik, M.; Huikuri, H.V.; Peng, C.K.; Schmidt, G.; Yamamoto, Y.; Gorenek, B.; Lip, G.Y.; et al. Advances in heart rate variability signal analysis: Joint position statement by the e-Cardiology ESC Working Group and the European Heart Rhythm Association co-endorsed by the Asia Pacific Heart Rhythm Society. *Europace* **2015**, *17*, 1341–1353. [CrossRef]
60. Friedrich, D.; Aubert, X.L.; Führ, H.; Brauers, A. Heart rate estimation on a beat-to-beat basis via ballistocardiography—A hybrid approach. In Proceedings of the 2010 Annual International Conference of the IEEE Engineering in Medicine and Biology, Buenos Aires, Argentina, 31 August–4 September 2010; pp. 4048–4051. [CrossRef]
61. Lahdenoja, O.; Hurnanen, T.; Tadi, M.J.; Pänkäälä, M.; Koivisto, T. Heart Rate Variability Estimation with Joint Accelerometer and Gyroscope Sensing. In Proceedings of the Computing in Cardiology, Vancouver, BC, Canada, 11–14 September 2016; Volume 43, pp. 717–720.
62. Laurin, A.; Blaber, A.; Tavakolian, K. Seismocardiograms return valid heart rate variability indices. In Proceedings of the Computing in Cardiology 2013, Zaragoza, Spain, 22–25 September 2013; pp. 413–416.
63. Rienzo, M.D.; Vaini, E.; Bruno, B.; Castiglioni, P.; Lombardi, P.; Parati, G.; Lombardi, C.; Meriggi, P.; Rizzo, F. Wearable Seismocardiography: Towards the beat-to-beat assessment of cardiac mechanics during sleep in microgravity. In Proceedings of the 2014 8th Conference of the European Study Group on Cardiovascular Oscillations (ESGCO), Trento, Italy, 25–28 May 2014; pp. 239–240. [CrossRef]
64. Munck, K.; Sørensen, K.; Struijk, J.J.; Schmidt, S.E. Multichannel seismocardiography: An imaging modality for investigating heart vibrations. *Physiol. Meas.* **2020**, *41*, 115001. [CrossRef]
65. Kaisti, M.; Tadi, M.J.; Lahdenoja, O.; Hurnanen, T.; Saraste, A.; Pankaala, M.; Koivisto, T. Stand-Alone Heartbeat Detection in Multidimensional Mechanocardiograms. *IEEE Sens. J.* **2019**, *19*, 234–242. [CrossRef]
66. Kaisti, M.; Tadi, M.J.; Lahdenoja, O.; Hurnanen, T.; Pänkäälä, M.; Koivisto, T. Mechanocardiograms with ECG Reference. IEEE DataPort. 2018. Available online: https://ieee-dataport.org/documents/mechanocardiograms-ecg-reference (accessed on 3 February 2023).
67. Yang, C.; Fan, F.; Aranoff, N.; Green, P.; Li, Y.; Liu, C.; Tavassolian, N. An Open-access Database for the Evaluation of Cardio-mechanical Signals from Patients with Valvular Heart Diseases (1.0). [Data set]. Zenodo. 2021. Available online: https://zenodo.org/record/5279448#.Y-tv3q1BxPY (accessed on 3 February 2023).
68. Shimmer. Shimmer3 (IMU) Wireless Sensor Platform Specifications. 2022. Available online: https://shimmersensing.com/wp-content/uploads/2022/04/Shimmer3-IMU-Spec-Sheet.pdf (accessed on 3 February 2023).

69. Yang, C.; Tavassolian, N. Combined Seismo- and Gyro-Cardiography: A More Comprehensive Evaluation of Heart-Induced Chest Vibrations. *IEEE J. Biomed. Health Inform.* **2018**, *22*, 1466–1475. [CrossRef]
70. Pan, J.; Tompkins, W.J. A Real-Time QRS Detection Algorithm. *IEEE Trans. Biomed. Eng.* **1985**, *BME-32*, 230–236. [CrossRef]
71. Sørensen, K.; Schmidt, S.E.; Jensen, A.S.; Søgaard, P.; Struijk, J.J. Definition of Fiducial Points in the Normal Seismocardiogram. *Sci. Rep.* **2018**, *8*, 15455. [CrossRef]
72. Vest, A.N.; Da Poian, G.; Li, Q.; Liu, C.; Nemati, S.; Shah, A.J.; Clifford, G.D. An open source benchmarked toolbox for cardiovascular waveform and interval analysis. *Physiol. Meas.* **2018**, *39*, 105004. [CrossRef]
73. Poian, G.D.; Li, Q.; Schwabedal, J. embar. cliffordlab/PhysioNet-Cardiovascular-Signal-Toolbox: PhysioNet-Cardiovascular-Signal-Toolbox 1.0.2. GitHub. 2019. Available online: https://zenodo.org/record/3358559#.Y-tphq1BxPY (accessed on 3 February 2023).
74. Lomb, N.R. Least-squares frequency analysis of unequally spaced data. *Astrophys. Space Sci.* **1976**, *39*, 447–462. [CrossRef]
75. Scargle, J.D. Studies in astronomical time series analysis. II—Statistical aspects of spectral analysis of unevenly spaced data. *Astrophys. J.* **1982**, *263*, 835. [CrossRef]
76. Ciccone, A.B.; Siedlik, J.A.; Wecht, J.M.; Deckert, J.A.; Nguyen, N.D.; Weir, J.P. Reminder: RMSSD and SD1 are identical heart rate variability metrics. *Muscle Nerve* **2017**, *56*, 674–678. [CrossRef] [PubMed]
77. Shaffer, F.; Ginsberg, J.P. An Overview of Heart Rate Variability Metrics and Norms. *Front. Public Health* **2017**, *5*, 258. [CrossRef] [PubMed]
78. Brennan, M.; Palaniswami, M.; Kamen, P. Do existing measures of Poincare plot geometry reflect nonlinear features of heart rate variability? *IEEE Trans. Biomed. Eng.* **2001**, *48*, 1342–1347. [CrossRef] [PubMed]
79. İşler, Y.; Kuntalp, M. Combining classical HRV indices with wavelet entropy measures improves to performance in diagnosing congestive heart failure. *Comput. Biol. Med.* **2007**, *37*, 1502–1510. . [CrossRef]
80. Kitlas Golińska, A. Poincaré Plots in Analysis of Selected Biomedical Signals. *Stud. Logic Gramm. Rhetor.* **2013**, *35*, 117–127. [CrossRef]
81. Ruan, X.; Liu, C.; Liu, C.; Wang, X.; Li, P. Automatic detection of atrial fibrillation using R-R interval signal. In Proceedings of the 2011 4th International Conference on Biomedical Engineering and Informatics (BMEI), Shanghai, China, 15–17 October 2011; Volume 2, pp. 644–647. [CrossRef]
82. Biala, T.; Dodge, M.; Schlindwein, F.S.; Wailoo, M. Heart rate variability using Poincaré plots in 10 year old healthy and intrauterine growth restricted children with reference to maternal smoking habits during pregnancy. In Proceedings of the 2010 Computing in Cardiology, Belfast, UK, 26–29 September 2010; pp. 971–974.
83. Kozak, M. What is Strong Correlation? *Teach. Stat.* **2009**, *31*, 85–86.
84. Arslan, U.; Özdemir, M.; Kocaman, S.A.; Balcıoğlu, S.; Cemri, M.; Çengel, A. Heart rate variability and heart rate turbulence in mild-to-moderate aortic stenosis. *EP Eur.* **2008**, *10*, 1434–1441.
85. Werner, B.; Piorecka-Makula, A.; Bobkowski, W. Heart rate variability in children with aortic valve stenosis—A pilot study. *Arch. Med. Sci.* **2013**, *9*, 535–539. [CrossRef]
86. Charlier, P.; Cabon, M.; Herman, C.; Benouna, F.; Logier, R.; Houfflin-Debarge, V.; Jeanne, M.; Jonckheere, J.D. Comparison of multiple cardiac signal acquisition technologies for heart rate variability analysis. *J. Clin. Monit. Comput.* **2019**, *34*, 743–752. [CrossRef]
87. NXP Semiconductors. MMA8451Q, 3-Axis, 14-bit/8-bit Digital Accelerometer Datasheet. 2017. Available online: https://www.nxp.com/docs/en/data-sheet/MMA8451Q.pdf (accessed on 3 February 2023).
88. Maxim Integrated. MAX21000 Ultra-Accurate, Low Power, 3-Axis Digital Output Gyroscope Datasheet. 2013. Available online: https://www.analog.com/media/en/technical-documentation/data-sheets/MAX21000.pdf (accessed on 3 February 2023).
89. Yang, C.; Ojha, B.; Aranoff, N.D.; Green, P.; Tavassolian, N. Classification of Aortic Stenosis Before and After Transcatheter Aortic Valve Replacement Using Cardio-mechanical Modalities. In Proceedings of the 2020 42nd Annual International Conference of the IEEE Engineering in Medicine Biology Society (EMBC), Montreal, QC, Canada, 20–24 July 2020; pp. 2820–2823. [CrossRef]